CrystEngComm

Dynamic Article Links

Cite this: *CrystEngComm*, 2012, **14**, 6833–6838

www.rsc.org/crystengcomm

PAPER

Design and growth of metamorphic InAs/InGaAs quantum dots for single photon emission in the telecom window

Luca Seravalli,* Giovanna Trevisi and Paola Frigeri

Received 30th May 2012, Accepted 26th July 2012
DOI: 10.1039/c2ce25860a

III-V semiconductor quantum dots are strong candidates for single photon sources and are fundamental cornerstones in the growing field of quantum cryptography and quantum computing. We present an original MBE growth approach, based on the deposition of sub-critical coverages of InAs on metamorphic InGaAs buffers, that allows us to obtain low surface densities for QDs emitting in the 1.3–1.55 μm telecom spectral window. Thanks to the unique properties of the metamorphic system, which allows us to independently change the QD strain and InGaAs buffer composition, we discuss how the sub-critical growth regime is fundamentally different from the widely known Stranski–Krastanow method. Moreover, we present the morphological and optical properties of these nanostructures, aiming to prove that they can be effective single photon sources emitting at 1.3–1.55 μm at low temperatures, thanks to the possibility of engineering the structures by using InGaAs capping layers at different compositions.

Introduction

The search for reliable single photon sources is strongly driven by the quest for the development of basic building blocks for quantum information devices.[1] III–V semiconductor self-assembled quantum dots (QDs) have already proved themselves as valuable sources for single and entangled photons for applications in the field of quantum cryptography, thanks to the possibility of integrating them into nanocavities and the ease of fabricating QD-based devices.[2–4] Moreover, InAs/GaAs QD nanostructures allow for the tuning of the emission wavelength in the 1.3–1.55 μm window, used for silica-based fiber optic telecom and datacom transmissions, a feature that has sparked a considerable amount of research in the last decade aimed towards the development of QD-based devices grown on GaAs substrates.[5–8] Hence, this system shows promise for the development of sources of single photons in telecom windows used for secure data transmission in silica optical fibers. However, the concomitant requirements of low QD densities (in the order of a few dots per μm) and a red-shifted emission are not easily met and in the last few years substantial research has been devoted to designing and growing InAs nanostructures on GaAs substrates with this aim.[9,10]

In particular, in this work we report the design and growth *via* Molecular Beam Epitaxy (MBE) of InAs/GaAs and metamorphic InAs/InGaAs QD nanostructures with emissions at 10 K in the range of 1.3–1.55 μm and with densities low enough for single QD characterization. To fulfil these requirements, we considered an original method proposed for the growth of InAs/GaAs QD structures[11] and here developed for the deposition of QDs on GaAs and InGaAs metamorphic buffers (MBs), relying on a growth regime that is different from the mainstream Stranski–Krastanow (SK) method as it is based on the deposition of a layer of InAs of sub-critical thickness (below the value for the SK transition), as is schematically presented in Fig. 1. In a previous publication, we presented the optical characterization of single QDs in these structures, proving how metamorphic quantum dots could be valuable candidates as single photon sources for long wavelength telecom windows.[12]

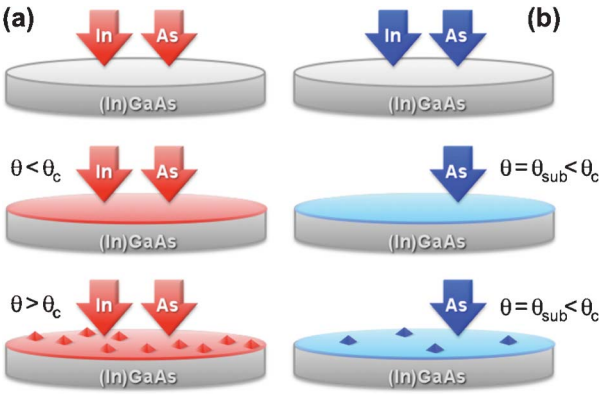

Fig. 1 Schematic representations of the Stranski–Krastanow growth (a) and of the sub-critical growth (b) of InAs QDs on (In)GaAs layers grown on GaAs (100) substrates. θ is the InAs coverage that builds up when both In and As fluxes, depicted as coloured arrows, impinge on the surface; θ_c indicates the SK critical InAs coverage for the 2D–3D transition while θ_{sub} indicates the sub-critical InAs coverage.

IMEM-CNR Institute, Parco Area delle Scienze, 37/a, 43124, Parma, Italy. E-mail: seravall@imem.cnr.it; Fax: +39-0521-269206; Tel: +39-0521-269210

Experimental

The structures were grown by Molecular Beam Epitaxy (MBE) on semi-insulating (100) GaAs substrates with a GaAs layer of 100 nm grown at 600 °C. For metamorphic structures, the growth proceeded at 400 °C with an $In_xGa_{1-x}As$ *meta*-buffer (MB) 500 nm thick and a thin GaAs layer of 5 nm grown by ALMBE (Atomic Layer Molecular Beam Epitaxy). After a growth interruption of 210 s to increase the substrate temperature, we deposited θ ML of InAs at 490 °C at 0.1 ML s^{-1} followed by a post-growth annealing (PGA) pause of time τ at the same temperature and under an As flux (with a beam equivalent pressure of 6×10^{-6} Torr). Finally, we capped the structure with 20 nm of $In_yGa_{1-y}As$ grown at 360 °C by ALMBE (where not explicitly mentioned, $y = x$). Similar structures were deposited directly onto the GaAs layer, following the same procedure.

MB compositions of $x = 0.15$, 0.22 and 0.30 were considered, resulting in a QD-MB mismatch of 6.34%, 5.80% and 5.19%, respectively, as calculated on the basis of the Mareè theory of strain relaxation,[14] whose predictions have been experimentally confirmed for InGaAs MBs by the different techniques shown in Ref. 15 and Ref. 16. Three values of x were chosen and the μ-PL data was obtained for $x = 0.15$ and 0.30, indicating that the QD emission in the 1.3 μm range can be obtained.[12] To study the QD properties as functions of x, we chose to add the $x = 0.22$ value that falls between 0.15 and 0.30.

Reflection High Energy Electron Diffraction (RHEED) patterns were used to determine the two-dimensional (2D) to three-dimensional (3D) InAs critical thickness (θ_c) on InGaAs MBs in the Stranski–Krastanow growth regime and to monitor the evolution of sub-critical layers during the PGA.[11] Atomic Force Microscopy (AFM) measurements of the uncapped structures were carried out in the contact-mode configuration. Continuous-wave photoluminescence (PL) was performed at 10 K. The excitation source was a 532 nm laser line with a maximum power density of about 5 W cm^{-2}. The PL spectra were measured by a Fast-Fourier Transform spectrometer with a 1 meV resolution and a cooled Ge detector.

Results and discussion

In order to investigate the growth process of InAs QDs on metamorphic InGaAs buffers whilst using the sub-critical thickness approach, a method not previously investigated in the literature for metamorphic structures, we monitored the evolution of the RHEED pattern from a streaky 2D to a spotty 3D pattern during the PGA. Thanks to the unique property of InGaAs MBs of providing structures where the QD-MB mismatch and surface composition can be changed independently,[13] we were able to obtain surfaces with different lattice parameters (determined by the MB characteristics) but with the same composition (imposed by the thin 5 nm GaAs layer grown over the MB). Hence, we have effectively realized a virtual GaAs buffer layer with an adjustable mismatch, f, which allows us to consider the dependence of the QD growth process on this fundamental parameter. In a previous publication,[13] we discussed in depth the dependence of θ_c on f and on the surface composition for the standard Stranski–Krastanow growth. Here, we will focus on the effect of changing f for the sub-critical growth regime of metamorphic quantum dots.

Although this growth method is relatively less explored, compared with the Stranski–Krastanow route, some reports have discussed the characteristics of this regime, highlighting in some cases that a kinetic mean-field theory can explain the formation of QDs *via* precursors which form during the wetting layer growth and then convert into QDs during the PGA,[11] while in other works it has been pointed out that this growth regime could be controlled by thermodynamics rather than kinetics.[17]

As a true transition thickness does not exist in this regime but rather a sub-critical InAs 2D layer that evolves in QDs, we chose to consider the minimal InAs coverage, θ_{sub}, that results in QD formation with fixed growth conditions, as a relevant quantity for each buffer composition (substrate temperature of 490 °C and 100 s PGA time). This value was obtained by growing structures with different InAs coverages in steps of 0.05 MLs, monitoring the RHEED pattern to observe the transition to a 3D spotty pattern during the PGA and verifying the actual QD formation by AFM characterization.

The data for these minimal InAs coverages, θ_{sub}, for structures grown directly on GaAs and $In_xGa_{1-x}As$ MBs covered by a thin GaAs layer are reported in Fig. 2 as "sub-critical", alongside the critical thickness, θ_c, for the structures grown in the Stranski–Krastanow regime with the same parameters, indicated as "SK". While the reduction of the mismatch induces an increase of both

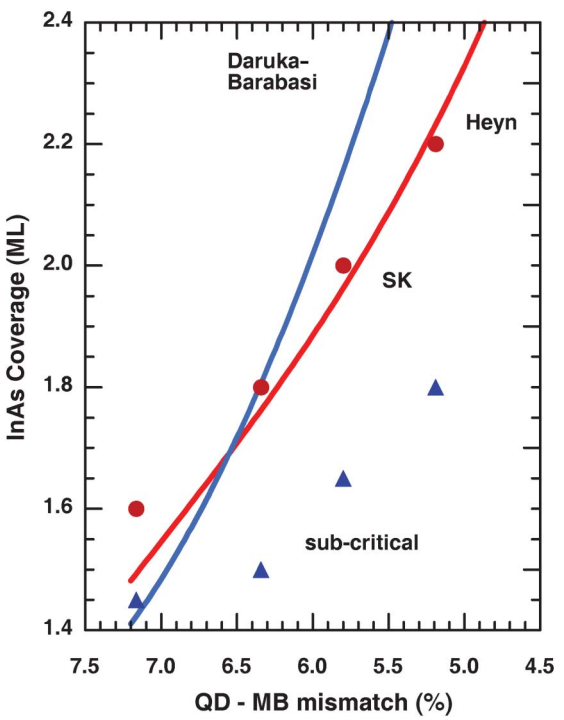

Fig. 2 2D–3D transition thickness, θ_c, for Stranski–Krastanow QDs (circles) and the minimal InAs coverage, θ_{sub}, resulting in QD formation for sub-critical QDs (triangles) as functions of the QD-MB mismatch. The solid line labelled "Heyn" represents model values from Ref. 18 while the solid line labelled "Daruka–Barabasi" represents model values from Ref. 19. Both have been rigidly shifted along the vertical axis to intercept the data.

θ_c and θ_{sub}, it is evident that the increase of θ_{sub} is less pronounced in comparison with θ_c.

This dependence of θ_c on the QD-MB mismatch has been considered in Ref. 13, where we show that this increase is explainable by the reduction of the elastic energy stored in the InAs 2D layer when the mismatch is lowered. As the driving force for the nucleation of 3D islands is the relief of this elastic strain energy, this means that a thicker 2D layer is necessary to reach the critical value of the strain energy which causes the nucleation of 3D islands. This is confirmed by the good agreement of the SK data with the kinetic rate model by Heyn,[18] also shown in Fig. 2 as the red line labelled "Heyn" (taken from Ref. 13). For the "sub-critical" data, however, it is evident that the above model does not agree with the experimental *f*- dependence, even though it has been shown that a kinetic model based on the mass transport between the wetting layer and the 2D precursor could reproduce the time evolution of the RHEED patterns for the sub-critical growth of InAs QDs on GaAs.[11] On the other hand, it has recently been argued that this growth regime can be simulated by an approach based on the thermodynamic equilibrium, a rather different approach from the kinetic-based methods.[17] In an effort to interpret our data, we considered the dependence of the critical thickness on *f*, as predicted by equilibrium models, and compared it with our experimental data. As specific examples for InAs/InGaAs do not exist, we considered the phase diagrams by Daruka and Barabasi[19] to extract the expected dependence of the critical thickness on the mismatch, which represents coverage values for the transition from a stable 2D layer to an unstable 2D layer evolving into 3D QDs. The calculation is shown as a blue solid line labelled "Daruka-Barabasi". It is evident that the equilibrium model calculation predicts a much larger increase in the critical thickness of the 2D–3D transition, even larger than SK QDs, and hence does not agree with the present experimental data. This indicates that neither a simple equilibrium picture nor a kinetic-based approach can explain in full the growth regime of sub-critical InAs QD formation. This suggests that other factors might be at play in this system, meaning this growth regime is rather different from the common SK method. It is worth noting that only the metamorphic system allows for the design and growth of structures where the mismatch, *f*, can be changed independently from the surface composition, allowing us to study in depth the effect of this parameter on QD growth. This should stimulate theoretical work on the sub-critical QD growth from a fundamental point of view.

Moreover, it is important to note that the sub-critical QD growth approach, avoiding the effects due to incoming In atoms, allows for an in-depth study of QD nucleation mechanisms in metamorphic structures which are related to the strain status and surface corrugation of the InGaAs buffer layers. To this aim we performed AFM measurements on the same QD structures investigated by RHEED (Fig. 2) after their removal from the MBE chamber. For this purpose, we optimized the substrate temperature quench method after the PGA in order to minimize any postgrowth changes and to preserve the surface morphologies for *ex situ* studies. Fig. 3 shows the top-view AFM micrographs for the $x = 0.15$, 0.22 and 0.30 samples with InAs coverages of θ_{sub} = 1.50, 1.65 and 1.80 ML, respectively. The AFM analysis reveals that the sub-critical approach, by fine-adjusting the InAs coverage

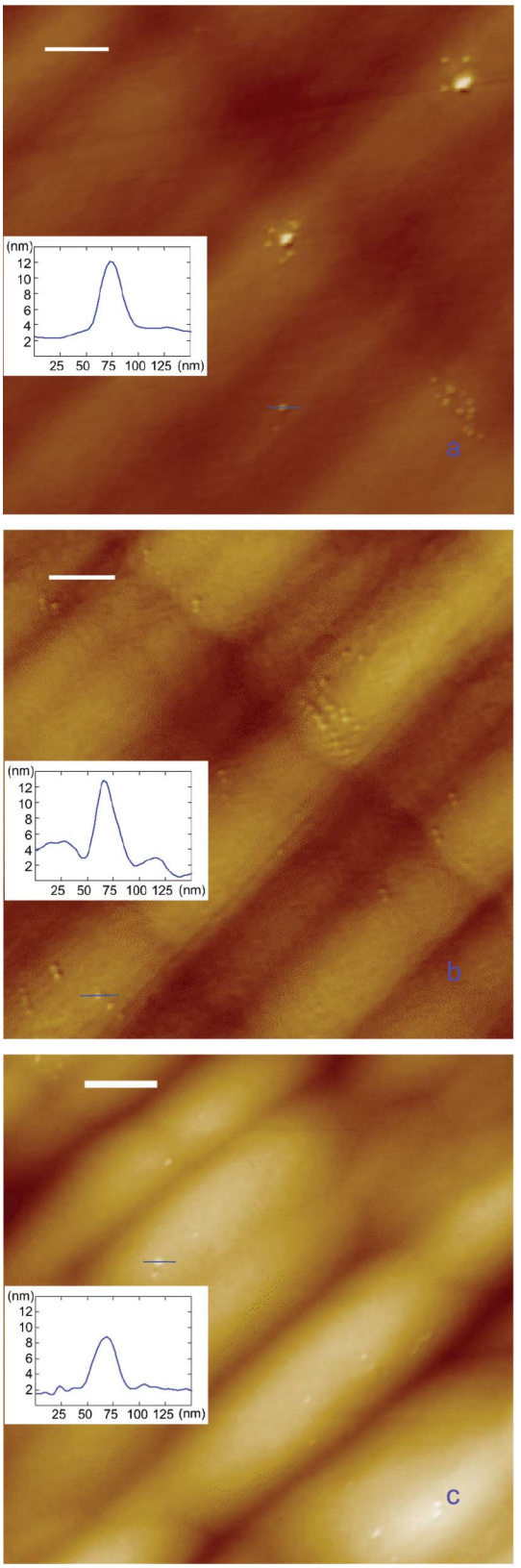

Fig. 3 2 μm × 2 μm AFM images (scale bar = 250 nm, height color scale 30 nm) of sub-critical QDs with parameters: a) $x = 0.15$, θ_{sub} = 1.50 ML and $\tau = 100$ s, b) $x = 0.22$, θ_{sub} = 1.65 ML and $\tau = 100$ s, c) x = 0.30, θ_{sub} = 1.80 ML and $\tau = 100$ s. The insets show AFM height profiles along the indicated lines.

and PGA times, allows us to obtain very low QD densities, in the 10^8 cm^{-2} range, suitable for single-dot studies. However, the measured density values cannot be directly compared due to the difference in the sub-critical InAs coverage needed to observe the 2D–3D transition during the substrate annealing process in structures with different MB compositions.

AFM measurements show also that metamorphic QD structures exhibit an undulated surface morphology, due to the corrugation of the growth-front during the deposition of the InGaAs layers.[13] Surface corrugation depends on x and affects the QD positioning and then the uniformity of the QD distribution on the InGaAs underlayer.

In particular, we observed that InAs islands nucleate preferentially on top of the ridge (x = 0.15) and mound-like (x = 0.22, 0.30) features oriented along the [$\tilde{1}$10] direction that dominate the morphology of the metamorphic structures. The disorder in the spatial distribution of InAs QDs on InGaAs results in non-uniform distances between neighbouring islands, changing the strain field on the surface and hence the electronic properties. Moreover, a corrugated surface morphology seems to favour the nucleation of islands with a relatively large size-dispersion which leads to broad, asymmetric PL spectra. The increase in the PGA time did not evidence any changes to these characteristic features and thus it can be concluded that the PGA does not substantially influence the QD density or size dispersion. The correlation between the morphological and PL characterizations is applicable since, due to the low capping temperature, we may suppose that the changes in island size during the overgrowth are small and the AFM data on size dispersion is still significant for capped structures.

We will now present and discuss the PL characterization of these metamorphic nanostructures, considering at first the effect of the increase of the PGA time, τ, on the ensemble emission spectra of QDs grown directly on GaAs, reported in Fig. 4 for τ = 20, 60 and 100 s. It can be shown that the PL emission is rather broad and weak, a normal feature for low density structures where the control of the homogeneity of the structures is not a primary concern as they are intended for single dot studies.

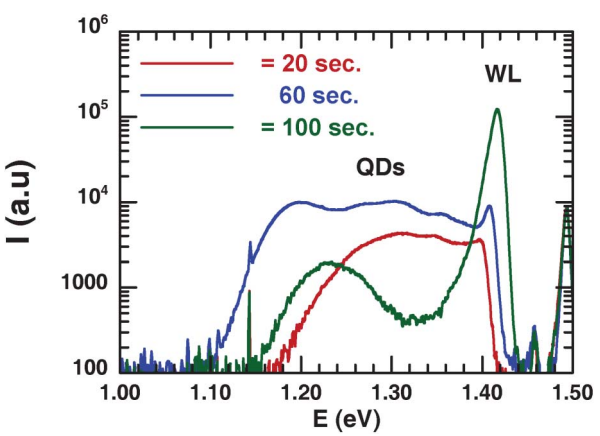

Fig. 4 10 K PL spectra for sub-critical InAs QDs deposited on GaAs for different PGA times. The PL features attributed to WL and QD are indicated.

The multi-peaked PL spectra correlate well with the QD ensembles with large size dispersions, as observed in the AFM data, giving rise to broadened spectra that span a wide range of wavelengths. The increase of τ causes an increase in the intensity of the InAs wetting layer (WL) emission and a slight modification of the shape of the PL spectrum, an effect also observed for QDs deposited on InGaAs MB. The latter feature could be explained by an enhancement of the surface migration of adatoms when larger τ are used and Ref. 20 discussed how the migration length can be gradually increased by increasing the annealing time during the QD formation. This could cause a change in the relative population of QDs with different sizes, with a slight red-shift of the peak emission for increased τ (at least for InAs deposited on GaAs). It is worth mentioning that the PGA on SK QDs has a very different effect: a blue-shift in the QD emission,[21] theoretically explained by a change in the chemical disorder and strain relief.[22] As a matter of fact, this different influence of the PGA on sub-critical QDs has already been observed.[20] The change in PGA time also had a similar effect on QDs grown on InGaAs MBs.

It is worth noting that, for the structure with a 100 s PGA, the emission intensity of the QDs is reduced by almost one order of magnitude. As the AFM data did not evidence any relevant changes in the QD density, we can explain this result by considering that the increase in the PGA time could cause a relative increase of large-sized QDs in comparison with small-sized QDs, as indicated by the slight red-shift of the PL peak emission. As discussed in Ref. 23, the occurrence of large-sized QDs is related to the ripening process: a fraction of these QDs could plastically relax and induce the formation of defects which act as non-radiative recombination centers, causing a reduction in the intensity of the PL emission of QD ensembles.

Representative PL spectra recorded at 10 K for the metamorphic structures are presented in Fig. 5 for structures with x = 0, 0.15, 0.22 and 0.30, with the spectra normalized at the QD peak emission. The values of θ_{sub} and τ are the values that allowed for the maximum red-shift of the emission: θ_{sub} = 1.50 ML and τ = 60 s for x = 0.15, θ_{sub} = 1.65 ML and τ = 100 s for x = 0.22,

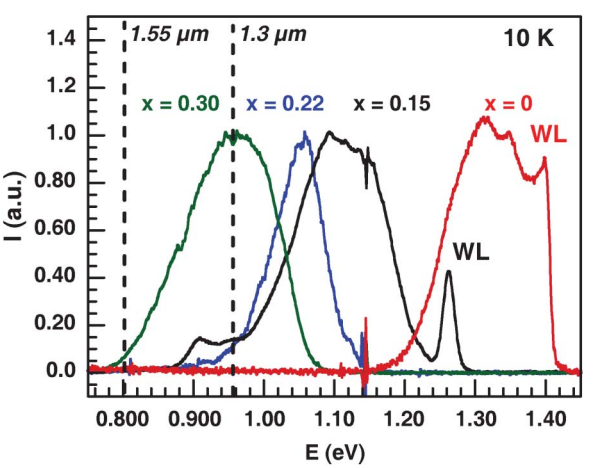

Fig. 5 10 K PL spectra for sub-critical InAs QDs deposited on InGaAs MBs and GaAs (indicated as x = 0). The PL features attributed to the WL and QDs are indicated alongside the energy values corresponding to the 1.3 μm and 1.55 μm emission.

θ_{sub} = 1.80 ML and τ = 300 s for x = 0.30. μ-PL studies on some of these structures have been presented elsewhere[12] and hence, we will focus on the ensemble studies to discuss in particular the effect of design parameters on the emission wavelength of QDs, aiming at red-shifting the emission towards 1.3 and 1.55 μm.

The first important observation is that the emission wavelength is red-shifted when x is increased, down to the important wavelength of 1.3 μm when $In_{0.30}Ga_{0.70}As$ MBs are used. As is widely discussed in Ref. 24 and Ref. 25, when the QD-MB mismatch is reduced, the QD strain is decreased causing a lowering of the QD energy gap. In the present case of the sub-critical deposition of InAs QDs, other effects, such as significant changes in the QD sizes and shapes and modified QD compositions cannot however be neglected as it was done for SK QDs.

It is also interesting to note that in Fig. 5, the WL emission is rather strong in structures with x = 0 and 0.15 while it is not observable for higher x values. This observation agrees with the results from other works on metamorphic QD structures grown with the standard SK growth method where, on the basis of PhotoReflectance and Photoluminescence Excitation spectroscopy characterizations, it was concluded that WL states are absent in high-x MBs.[26,27] This fact is of particular relevance for low-density metamorphic structures, where QDs are investigated as possible single photon sources in the telecom range. Indeed, it is now well established that WL states, besides affecting the thermal escape of carriers from QDs, also have relevant influences on confined carrier properties, such as oscillator strengths, inter-dot coupling and dipole polarization *via* Coulomb interactions, of fundamental relevance for single photon emission and control.[28,29]

In order to reach the important 1.55 μm emission, it is necessary to further red-shift the QD peak energy in the x = 0.30 structures. However, from Fig. 4 it is evident that increasing τ cannot be considered as a viable method for a consistent red-shift in the QD emission in metamorphic low density QD structures. Henceforth, to further red-shift the QD emission energy towards the 1.55 μm range, we grew structures with $In_yGa_{1-y}As$ capping layers where $y > x$. It is important to note that the thickness of this capping layer (20 nm) is lower than the critical thickness for the plastic relaxation of the compressive strain energy that builds up in the $In_yGa_{1-y}As$ layer due to the mismatch with the $In_xGa_{1-x}As$ MB. This is an important consideration when using $In_yGa_{1-y}As$ capping layers to red-shift the QD emission.[10] The effect on the PL peak energy is shown in Fig. 6(a) for structures with x = 0.22 and x = 0.30. It is noteworthy that the emission energies of the x = 0.30 samples span the whole 1.3–1.55 μm range, even exceeding the latter value when y = 0.60 capping layers are used, as shown in Fig. 6(b). As discussed in depth in Ref. 10, the cap-induced red-shift may be due to different effects, namely the reduction of band discontinuities that confine carriers, the decrease in QD strain and a possible change in QD size or composition.

From the above results, it is evident that the emission energy of metamorphic low-density QDs can be controlled in the 1.3–1.55 μm range by using adequate x and y values. It is also important to note that it is well-known that structures with MB have defects related to the plastic relaxation of the compressive strain of thick InGaAs layers. Notwithstanding this, many methods can be used to consistently reduce the density of defects in the proximity of QDs in these metamorphic nanostructures,

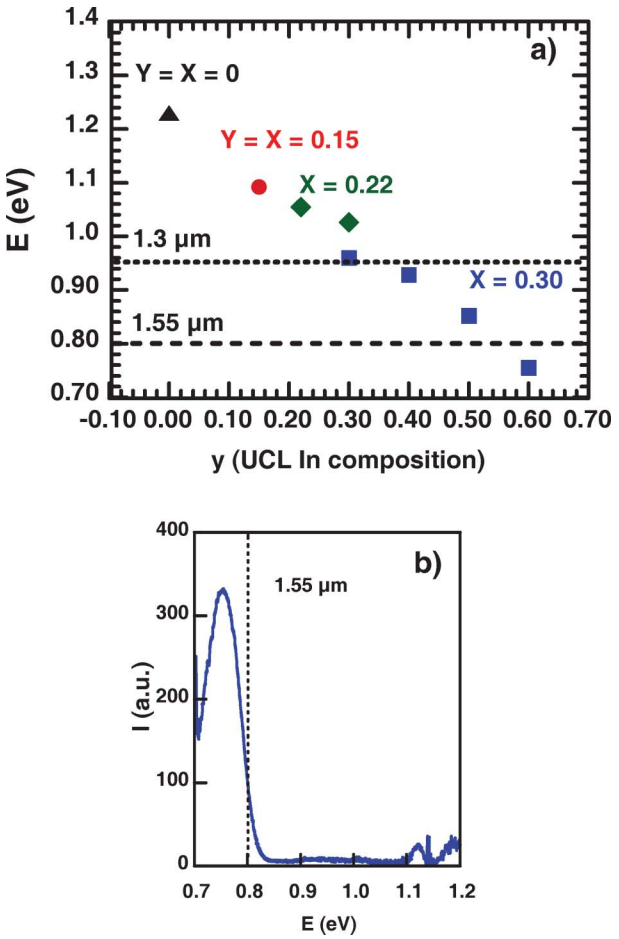

Fig. 6 a) 10 K PL peak emission energies of QDs as a function of In composition of the $In_yGa_{1-y}As$ capping layer for different In compositions of the $In_xGa_{1-x}As$ MBs: x = 0.15 (circles), 0.22 (diamonds), 0.30 (squares) and for QDs deposited on GaAs (triangles). The energy values corresponding to 1.3 μm and 1.55 μm emissions are indicated by dashed horizontal lines. b) 10 K PL spectrum for sub-critical InAs QDs deposited on $In_{0.30}Ga_{0.70}As$ MB and capped by a $In_{0.60}Ga_{0.40}As$ layer.

allowing for MB-based structures for QD photonic applications. Methods include the use of InGaAs graded buffers,[30] defect-filters based on QDs[31] and ad-hoc defect reduction techniques.[32] Therefore, also on the basis of the μ-PL characterization of these structures,[12] it is possible to conclude that metamorphic InAs QDs are suitable candidates to obtain single quantum dot emissions at long wavelengths on GaAs substrates.

Conclusions

We have designed, grown by MBE and characterized by AFM and PL metamorphic QD nanostructures with low QD densities (in the order of 10^8 cm^{-2}). The structures were prepared by depositing sub-critical coverages of InAs onto $In_xGa_{1-x}As$ metamorphic buffers followed by PGA, an approach that has thus far not been used for the preparation of structures aimed at single photon emissions in 1.3–1.55 μm telecom windows. By monitoring the time evolution of the RHEED pattern we were able to derive the minimal coverage, θ_{sub}, resulting in 3D island formation during the PGA stage. Thanks to the unique property

of the metamorphic system which allows for independent control of the QD-MB mismatch, f, and the surface composition, we were able to study the dependence of θ_{sub} on f and we conclude that the sub-critical growth process is intrinsically different from the Stranski–Krastanow method. Moreover, we have shown that the experimental f-dependence of θ_{sub} does not agree with the dependence expected by available model calculations based on kinetic-rate models and thermodynamic equilibrium models. Thus, this indicates that, besides the interest for growing QD-based structures for photonic applications in telecom windows, the metamorphic QD system allows us to check different QD growth theories thanks to the unique ability of independently changing the strain and composition.

From AFM characterizations, we demonstrated that sub-critical QD growth is a useful approach to fine control the density of metamorphic QDs in the low-density range. We studied the x-dependent morphological differences in InGaAs surface corrugation and their effects on QD positioning and on the uniformity of QD distribution. Preferential sites for island formation, driven by the strain and curvature of the starting InGaAs surfaces, were observed.

The analysis of the PL spectra allowed us to study the effect of the PGA time, indicating that an increase in the migration length of adatoms, related to the increase of τ, results in the change of distribution of different families of QDs and an increase of the emission efficiency of WLs. Moreover, we observed that in structures with high-x values, no PL emission from the WL is observable, indicating that the WLs might not be well-formed. This feature has interesting consequences for WL-QD carrier interactions, fundamental for single photon emission and manipulation from QDs.

From the optical characterization of these structures, we proved that it is possible to grow QDs which emit at long wavelengths on InGaAs buffers, up and beyond the 1.55 μm range, thanks to the possibility of engineering the structures by using $In_yGa_{1-y}As$ capping layers where $y > x$.

We believe these results show that metamorphic quantum dots are interesting nanostructures both from a fundamental point of view, in particular as a test system for advanced theoretical modelling of QD growth, and from an application perspective as they could allow for the development of single photon sources emitting at 1.3–1.55 μm at low temperatures.

Acknowledgements

We acknowledge the support of the Italian FIRB Project "Nanotecnologie e Nanodispositivi per la Società dell'Informazione" and by the "SANDiE" Network of Excellence of EC, Contract No. NMP4-CT-2004-500101. The AFM characterization was carried out at CIM, Parma University.

References

1 M. Eisaman, J. Fan, A. Migdall and S. Polyakov, *Rev. Sci. Instrum.*, 2011, **82**, 071101.
2 P. Petroff, *Adv. Mater.*, 2011, **23**, 2372–2376.
3 R. Stevenson, R. Young, P. Atkinson, K. Cooper, D. Ritchie and A. Shields, *Nature*, 2006, **439**, 179–182.
4 C. Salter, R. Stevenson, I. Farrer, C. Nicoll, D. Ritchie and A. Shields, *Nature*, 2010, **465**, 594–597.
5 R. Murray, D. Childs, S. Malik, P. Siverns, C. Roberts, J. Hartmann and P. Stavrinou, *Jpn. J. Appl. Phys.*, 1999, **38**, 528–530.
6 I. Sellers, H. Liu, M. Hopkinson, D. Mowbray and M. Skolnick, *Appl. Phys. Lett.*, 2003, **83**, 4710–4712.
7 H. Liu, Y. Qiu, C. Jin, T. Walther and A. Cullis, *Appl. Phys. Lett.*, 2008, **92**, 111906.
8 L. Seravalli, P. Frigeri, G. Trevisi and S. Franchi, *Appl. Phys. Lett.*, 2008, **92**, 213104.
9 L. Li, N. Chauvin, G. Patriarche, B. Alloing and A. Fiore, *J. Appl. Phys.*, 2008, **104**, 083508.
10 G. Trevisi, L. Seravalli, P. Frigeri and S. Franchi, *Nanotechnology*, 2009, **20**, 415607.
11 H. Song, T. Usuki, Y. Nakata, N. Yokoyama, H. Sasakura and S. Muto, *Phys. Rev. B: Condens. Matter Mater. Phys.*, 2006, **73**, 115327.
12 L. Seravalli, G. Trevisi, P. Frigeri, D. Rivas, G. Munoz-Matutano, I. Suarez, B. Alen, J. Canet and J. Martinez-Pastor, *Appl. Phys. Lett.*, 2011, **98**, 173112.
13 L. Seravalli, G. Trevisi and P. Frigeri, *CrystEngComm*, 2012, **14**, 1155–1160.
14 P. Maree, J. Barbour, J. Vanderveen, K. Kavanagh, C. Bulle-Lieuwma and M. Viegers, *J. Appl. Phys.*, 1987, **62**, 4413–4420.
15 V. Bellani, C. Bocchi, T. Ciabattoni, S. Franchi, P. Frigeri, P. Galinetto, M. Geddo, F. Germini, G. Guizzetti, L. Nasi, M. Patrini, L. Seravalli and G. Trevisi, *Eur. Phys. J. B*, 2007, **56**, 217–222.
16 M. Geddo, G. Guizzetti, M. Patrini, T. Ciabattoni, L. Seravalli, P. Frigeri and S. Franchi, *Appl. Phys. Lett.*, 2005, **87**, 263120.
17 G. Zhou, Y. Chen, J. Yu, X. Zhou, X. Ye, P. Jin and Z. Wang, *Appl. Phys. Lett.*, 2011, **98**, 071914.
18 C. Heyn, *Phys. Rev. B: Condens. Matter*, 2001, **64**, 165306.
19 I. Daruka and A. Barabasi, *Phys. Rev. Lett.*, 1997, **79**, 3708–3711.
20 C. Huang, T. Ou, S. Chou, M. Wu, S. Lin and J. Chi, *IEEE Trans. Nanotechnol.*, 2007, **6**, 589–594.
21 R. Leon, Y. Kim, C. Jagadish, M. Gal, J. Zou and D. Cockayne, *Appl. Phys. Lett.*, 1996, **69**, 1888–1890.
22 R. Santoprete, P. Kratzer, M. Scheffler, R. Capaz and B. Koiller, *J. Appl. Phys.*, 2007, **102**, 023711.
23 P. Frigeri, L. Nasi, M. Prezioso, L. Seravalli, G. Trevisi, E. Gombia, R. Mosca, F. Germini, C. Bocchi and S. Franchi, *J. Appl. Phys.*, 2007, **102**, 083506.
24 L. Seravalli, P. Frigeri, M. Minelli, P. Allegri, V. Avanzini and S. Franchi, *Appl. Phys. Lett.*, 2005, **87**, 063101.
25 L. Seravalli, M. Minelli, P. Frigeri, S. Franchi, G. Guizzetti, M. Patrini, T. Ciabattoni and M. Geddo, *J. Appl. Phys.*, 2007, **101**, 024313.
26 L. Seravalli, G. Trevisi, P. Frigeri, S. Franchi, M. Geddo and G. Guizzetti, *Nanotechnology*, 2009, **20**, 275703.
27 L. Seravalli, G. Trevisi, P. Frigeri, R. J. Royce and D. J. Mowbray, *J. Appl. Phys.*, 2012.
28 N. Chauvin, C. Zinoni, M. Francardi, A. Gerardino, L. Balet, B. Alloing and L. Li, *Phys. Rev. B: Condens. Matter Mater. Phys.*, 2009, **80**, 241306.
29 M. Winger, T. Volz, G. Tarel, S. Portolan, A. Badolato, K. Hennessy, E. Hu, A. Beveratos, J. Finley, V. Savona and A. Imamoglu, *Phys. Rev. Lett.*, 2009, **103**, 207403.
30 I. Tangring, H. Ni, B. Wu, D. Wu, Y. Xiong, S. Huang, Z. Niu, S. Wang, Z. Lai and A. Larsson, *Appl. Phys. Lett.*, 2007, **91**, 221101.
31 Z. Mi and P. Bhattacharya, *IEEE J. Sel. Top. Quantum Electron.*, 2008, **14**, 1171–1179.
32 L. Karachinskii, T. Kettler, I. Novikov, Y. Shernyakov, N. Gordeev, M. Maksimov, N. Kryzhanovskaya, A. Zhukov, E. Semenova, A. Vasil Ev, V. Ustinov, G. Fiol, M. Kuntz, A. Lochmann, O. Schulz, L. Reissmann, K. Posilovic, A. Kovsh, S. Mikhrin, V. Shchukin, N. Ledentsov and D. Bimberg, *Semicond. Sci. Technol.*, 2006, **21**, 691–696.